

A shared structural solution for neutralizing ebolaviruses

João M Dias^{1,7}, Ana I Kuehne^{2,7}, Dafna M Abelson¹, Shridhar Bale¹, Anthony C Wong³, Peter Halfmann⁴, Majidat A Muhammad², Marnie L Fusco¹, Samantha E Zak², Eugene Kang², Yoshihiro Kawaoka^{4,5}, Kartik Chandran³, John M Dye² & Erica Ollmann Saphire^{1,6}

Sudan virus (genus *Ebolavirus*) is lethal, yet no monoclonal antibody is known to neutralize it. We here describe antibody 16F6 that neutralizes Sudan virus and present its structure bound to the trimeric viral glycoprotein. Unexpectedly, the 16F6 epitope overlaps that of KZ52, the only other antibody against the GP_{1,2} core to be visualized to date. Furthermore, both antibodies against this crucial epitope bridging GP1–GP2 neutralize at a post-internalization step—probably fusion.

Ebolaviruses (family *Filoviridae*) cause severe hemorrhagic fever with up to a 90% fatality rate. Five antigenically distinct ebolaviruses have been identified that differ in genomic sequence by ~35–45%: Sudan, Ebola, Tai Forest, Reston and Bundibugyo. However, almost all human deaths result from infection with either Sudan virus (SUDV, formerly known as *Sudan ebolavirus*) or Ebola virus (EBOV, formerly known as *Zaire ebolavirus*). In October 2000 a new variant of SUDV, termed Gulu (SUDV-Gul)¹, emerged in the Gulu district of northwestern Uganda. It triggered the largest outbreak of Ebola hemorrhagic fever yet described, involving at least 425 people, of whom 224 died². Multiple monoclonal antibodies against EBOV have been developed^{3–7}, but very few of them are known to neutralize EBOV, and none of them neutralizes SUDV. Development and characterization of SUDV-specific monoclonal antibodies is essential for developing successful diagnostic reagents, immunotherapeutics and vaccines. Hence, we set out to raise monoclonal antibodies against SUDV and to structurally map their epitopes on the viral glycoprotein.

The cellular entry of ebolaviruses is a multistep process that includes attaching to target cells, internalizing into endosomes and fusing with endosomal membranes. The ebolavirus surface glycoprotein GP_{1,2} is the sole virus protein responsible for these processes. GP_{1,2} is expressed as a 676–amino acid precursor that is post-translationally cleaved by furin to yield two subunits, GP1 and GP2 (ref. 8). GP1 and GP2 remain covalently linked by a disulfide bond⁹,

and the resulting GP1–GP2 pair trimerizes to form a ~450-kDa envelope spike on the viral surface. GP1 is responsible for attaching the virus to new host cells, whereas GP2 mediates fusion of the virus envelope with cellular endosomal membranes. GP1 contains base, head, glycan-cap and mucin-like domains. The head subdomain contains putative receptor-binding regions and is capped by the heavily glycosylated glycan-cap and mucin-like domains. In the endosome, a flexible loop containing GP1 residues 190–213 is cleaved by host cathepsins^{10,11}. This cleavage releases the glycan-cap and mucin-like domains from GP1. Also in the endosome, GP2 releases from GP1 and undergoes irreversible conformational changes that drive fusion with host endosomal membranes. GP2 contains an N-terminal peptide, a hairpin-forming fusion loop and two heptad repeats connected by a functionally important linker. The first heptad repeat of GP2 is wound around the base of GP1 in a metastable, prefusion-specific conformation (Supplementary Fig. 1).

To generate antibodies specific for SUDV, we vaccinated BALB/c laboratory mice with Venezuelan equine encephalitis virus (VEEV) replicons bearing SUDV (strain Boniface) GP_{1,2} and boosted them with γ -radiation-inactivated SUDV-Boniface. We found that among the resulting monoclonal antibodies, IgG₁ 16F6 was directed against a conformational epitope on GP_{1,2}, was specific for SUDV and reacted with at least two different SUDV variants, Boniface and Gulu. We crystallized a trimeric complex of SUDV-Gulu GP_{1,2} in complex with a 16F6 Fab fragment in order to map the epitope of 16F6 and understand its SUDV specificity.

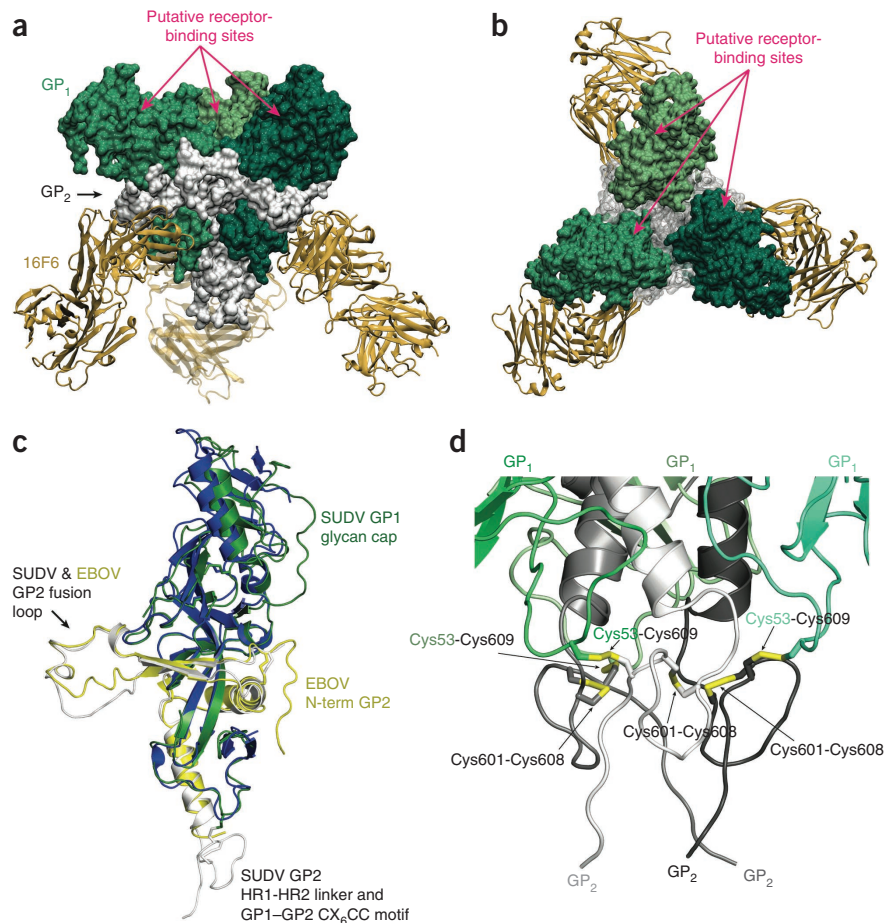
We expressed SUDV-Gulu GP_{1,2} for crystallization by transiently transfecting human embryonic kidney 293T cells. No mutations of the N-linked glycosylation sites were necessary, in contrast to previous studies that required these mutations for crystallization of EBOV GP_{1,2} (refs. 12,13). SUDV-Gulu GP_{1,2}–16F6 crystallized in the space group *I*23 with one monomeric GP_{1,2}–Fab complex in the asymmetric unit (Supplementary Methods and Supplementary Table 1). The biologically relevant trimer was formed by crystallographic symmetry, and GP_{1,2} was in its supposed metastable, prefusion conformation (Fig. 1).

In general, the SUDV GP_{1,2} crystals are more well-ordered than those of EBOV GP_{1,2}, allowing visualization of outer portions of the glycan cap and the linker region between the N- and C-terminal heptad repeats of GP2, neither of which were previously observed (Fig. 1c)¹³. The linker region contains a CX₆CC motif, in which the first two cysteines—Cys601 and Cys608—form an intra-GP2 disulfide bond that anchors the intervening polypeptide in a cloverleaf loop (Fig. 1d). The third cysteine (Cys609) anchors the GP2 cloverleaf to

¹Department of Immunology and Microbial Science, The Scripps Research Institute, La Jolla, California, USA. ²Division of Virology, United States Army Medical Research Institute of Infectious Diseases, Fort Detrick, Maryland, USA. ³Department of Microbiology and Immunology, Albert Einstein College of Medicine, Bronx, New York, USA. ⁴Department of Pathobiological Sciences, School of Veterinary Medicine, University of Wisconsin, Madison, Wisconsin, USA. ⁵Department of Special Pathogens, International Research Center for Infectious Diseases, Institute of Medical Science, University of Tokyo, Tokyo, Japan. ⁶The Skaggs Institute for Chemical Biology, The Scripps Research Institute, La Jolla, California, USA. ⁷These authors contributed equally to this work. Correspondence should be addressed to J.M. Dye (john.m.dye1@us.army.mil) and E.O.S. (erica@scripps.edu).

Received 13 April; accepted 6 September; published online 20 November 2011; doi:10.1038/nsmb.2150

Figure 1 Structure of Sudan virus (SUDV) GP_{1,2} in complex with Fab 16F6. GP1 subunits are shown in three different shades of green, GP2 subunits are white and bound 16F6 Fab fragments are gold. (a) Side view with viral membrane toward bottom and target cell toward the top. 16F6 binds the base of the GP_{1,2} peplomer, distal from putative receptor-binding sites. (b) Top view, from the perspective of the target cell. Putative receptor-binding sites are indicated by pink arrows. (c) Superposition of the SUDV and Ebola virus (EBOV) GP_{1,2} monomers. SUDV GP1–GP2 is shown in green for GP1 and white for GP2, and EBOV GP1–GP2 is shown in blue for GP1 and yellow for GP2. The SUDV structure includes additional regions of the glycan cap (top), the linker between heptad repeats 1 and 2 (HR1 and HR2) and the CX₆CC motif (bottom), although the N terminus of GP2 is disordered. (d) The linker region between HR1 and HR2 forms two disulfide bonds per monomer, one linking GP1 to GP2 (Cys53–Cys609) and one within GP2 (Cys601–Cys608). All figures were generated with PyMOL and VMD.



Cys53 in the base of GP1 (**Fig. 1d**). The shape and location of these disulfide-anchored loops suggest that they restrict the flexibility between N-terminal and C-terminal heptad repeats to an elbow-like range of motion, perhaps coupling the rotation of GP1 with the movement of the second heptad repeat of GP2 during membrane fusion.

The N-terminal half of the GP2 fusion loop is only 33% conserved between the two viruses and adopts a different, lower-hanging conformation (**Fig. 1c**). By contrast, the C-terminal half of the fusion loop is conserved in sequence and structure between SUDV and EBOV, and it is anchored to the outside of the trimer by Arg89 of the neighboring monomer's GP1-head subdomain (**Supplementary Fig. 2**). In SUDV, Arg89 forms five hydrogen bonds and a hydrophobic contact to the fusion loop. These contacts are conserved between SUDV and EBOV structures, and Arg89 is probably critical for clamping the fusion loop in place to anchor the trimer in its prefusion conformation (**Supplementary Fig. 2a**).

In the proposed three-dimensional receptor-binding site of GP1 (head subdomain), regions that project are conserved in sequence,

whereas regions that are recessed differ in sequence between SUDV and EBOV (**Fig. 2a** and **Supplementary Figs. 3** and **4**). The conserved, projecting regions (residues 114–120, 144–147, 149 and 172–173) may thus delineate surfaces expected to bind to the shared receptor.

More of the cathepsin-cleavage-site polypeptide is visible in the SUDV structure than in the EBOV structure. The position of the newly observed residues (190–192 and 212–213) immediately above and below the fusion loop suggests that the GP2 fusion loop could be tethered by the 190–213 polypeptide (**Supplementary Fig. 2b**). Regions of GP_{1,2} that surround the cathepsin cleavage site and that

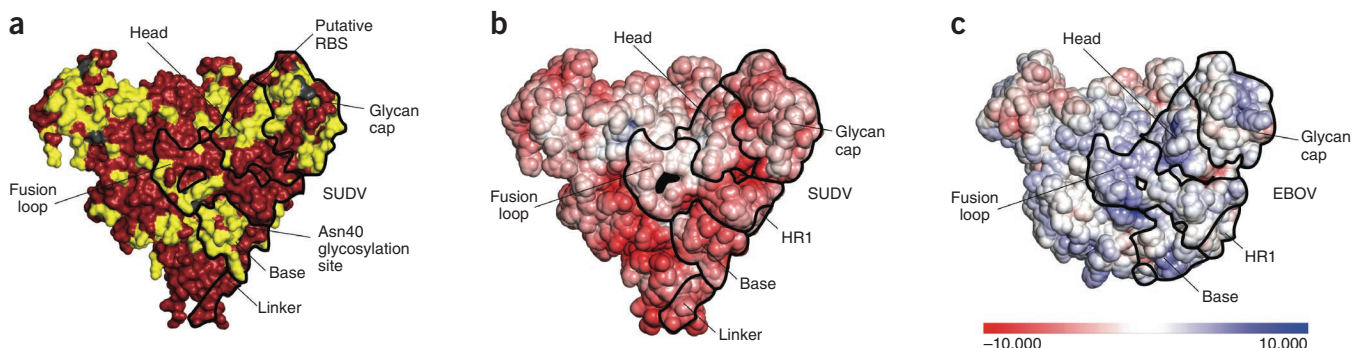
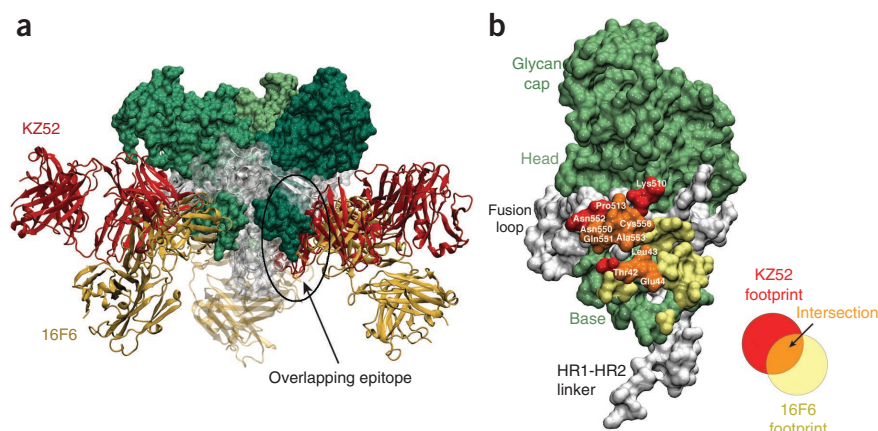


Figure 2 Surfaces of SUDV GP1. (a) Sequence conservation. Residues that are identical for both SUDV and EBOV are shown in red, and those that are different are shown in yellow. The domains of one GP_{1,2} monomer are outlined in black, with subdomains indicated. RBS, probable receptor-binding site. (b) Electrostatic potential representation of the SUDV GP_{1,2} surface with limits of $\pm 10k_B T/e_c$. (c) Electrostatic potential representation of the EBOV GP_{1,2} surface with limits of $\pm 10k_B T/e_c$.

Figure 3 16F6 epitope. (a) mAbs 16F6 and KZ52 recognize similar epitopes that bridge GP1–GP2 (black oval). Here, the structure of SUDV GP_{1,2} in complex with 16F6 (gold) is superimposed on the structure of EBOV GP_{1,2} in complex with KZ52 (brick red). For clarity, only the SUDV GP_{1,2} trimer (green and white) is shown. (b) Epitope footprints of 16F6 (yellow) and KZ52 (red) are mapped onto the SUDV surface. Residues shared between the two antibody epitopes (Thr42, Leu43, Glu44, Pro513, Asn550, Gln551, Asn552, Ala553 and Cys556) are shown in orange. A single GP_{1,2} monomer is shown in green for GP1 and white for GP2



line the trimer interface differ in sequence between SUDV and EBOV. Unexpectedly, these sequence variations cause distinctly different electrostatic charges in the GP_{1,2} peplomers. SUDV GP_{1,2} is acidic overall, especially at the base of the trimer where the metastable GP_{1,2} assembly intertwines. By contrast, EBOV GP_{1,2} is more neutral and is slightly basic where GP1 and GP2 intertwine (Fig. 2b,c and Supplementary Fig. 3).

The crystal structure reveals that mAb 16F6 binds to the base of the SUDV GP_{1,2} trimer and directly connects the base of GP1 to the stem of the internal fusion loop of GP2 (Fig. 1 and Supplementary Fig. 2c). Unexpectedly, the epitope of 16F6 overlaps that of mAb KZ52, thus far the only other antibody against the core of any ebolavirus GP_{1,2} to be structurally mapped¹³ (Fig. 3). KZ52 is specific for EBOV GP_{1,2} and was previously identified in a library derived from a human survivor of the 1995 outbreak in Kikwit, Zaire³. The 16F6 and KZ52 epitopes have the central nine residues in common: 42–44 of GP1 and 513, 550–553 and 556 of GP2 (Fig. 3b). Six of these nine residues are conserved between SUDV and EBOV (Supplementary Fig. 4). Fundamentally, although the two antibodies were produced against distinct viruses and in different immunological contexts (one by a vaccinated mouse and the other by a naturally infected human), these antibodies both recognized overlapping epitopes and arrived at a shared structural solution for neutralizing ebolaviruses.

In our study, 16F6 recognized native GP_{1,2} on the surface of cells infected with Sudan virus (Supplementary Fig. 5a,e). Plaque reduction neutralization tests (PRNT) illustrated that 16F6 confers a >99% reduction of SUDV plaques (100 plaque-forming units (PFUs)) at 20 μg ml⁻¹ (Supplementary Fig. 5b,e). Plaque reduction occurred in the presence or absence of the complement, indicating that binding of 16F6 alone was sufficient to block SUDV infection *in vitro*. Furthermore, intraperitoneal treatment of SCID mice with 100 μg of 16F6 every 5 d after SUDV infection delayed the death of mice by ~4 d ($P < 0.0001$; see Supplementary Fig. 5c,e).

We pseudotyped SUDV or EBOV GP_{1,2} onto vesicular stomatitis Indiana virus (VSIV) to allow a direct comparison of the ability of 16F6 and KZ52 to neutralize otherwise identical virions carrying the cognate surface antigen for each antibody. The neutralization activity of 16F6 was somewhat better than that of KZ52: >99% versus ~90% reduction in 293T cell transduction at equal concentrations (Supplementary Fig. 5d). Improvements in neutralization capacity are critical for providing immunotherapeutics against ebolaviruses, doses of a single PFU of which can be lethal to primates.

We conducted separate attachment and internalization assays, and these indicated that GP_{1,2}-pseudotyped VSIV attach to and enter Vero E6 cells even in the presence of saturating quantities of

16F6 or KZ52 (Supplementary Fig. 6a), and that KZ52 neutralizes VP30-deleted, biologically contained EBOV¹⁴ at a post-entry step (see Supplementary Fig. 6b; a biologically contained Sudan virus is not yet available). Consequently, antibodies against the shared 16F6 and KZ52 site must neutralize at a post-attachment, post-internalization step. Another step in the ebolavirus life cycle is cleavage of GP1 by cathepsins in the endosome^{15,16}. However, in our study, neither 16F6 nor KZ52 inhibited cathepsin L cleavage of either recombinant or viral surface GP1. Even in the presence of a ten-fold molar excess of KZ52 and 16F6, SUDV and EBOV GP_{1,2} were fully digested by cathepsin L within 30 min and 60 min, respectively (Supplementary Fig. 7).

Because 16F6 and KZ52 were found to function after internalization and did not inhibit cathepsin L cleavage, we think two possible mechanisms of inhibition remain: 16F6 and KZ52 may inhibit the function of some other unidentified factor, such as a co-receptor, or 16F6 and KZ52 may prevent the conformational changes in GP_{1,2} required for membrane fusion. Our structural evidence supports the latter: both 16F6 and KZ52 physically link GP1 to GP2 and are specific for their prefusion conformation. Furthermore, the conformational changes in GP2 required for membrane fusion cannot occur while 16F6 or KZ52 remain bound. Indeed, the greater neutralization capacity of 16F6 may be related to its more effective linkage of GP1 to GP2. The GP_{1,2} surface buried by 16F6 binding is composed of 60% GP1 and 40% GP2. By contrast, the GP_{1,2} surface buried by KZ52 is composed of 20% GP1 and 80% GP2. We think it is important to note that these antibodies are likely to remain bound to GP_{1,2} in the endosome: crystals of the EBOV GP_{1,2}-KZ52 complex generated at pH 4.8 show unit-cell dimensions and space group identical to those of complexes developed at neutral or basic pH¹², and GP_{1,2} pretreated at pH 5.0 is well recognized by KZ52 (ref. 13). Hence, pH alone is insufficient to separate GP1 from GP2.

This more well-ordered GP_{1,2} structure allowed us to predict conformational rearrangements that may occur during membrane fusion of all ebolaviruses. Arg89 is proximal to the proposed receptor-binding site in the GP1 head. Its hold on the neighboring monomer's fusion loop must be released for fusion to occur, an action that could be accomplished directly by receptor binding or indirectly by conformational change that is transmitted through neighboring residues that bind receptor, or it could occur by continued enzymatic processing of GP1. Subsequent unwinding of the fusion loops from the outside of the trimer could be facilitated by cathepsin cleavage of the 190–213 loop, which may loosely tether GP2 in place (Supplementary Fig. 2b). Motion of the fusion loops may be coupled to unwinding of the C-terminally linked heptad repeat 1 (HR1) from its GP1 spool

into its single, extended post-fusion helix^{17,18} and to the subsequent rotation of HR2 toward the target cell to form a six-helix bundle (Supplementary Fig. 1).

Antibodies against the fusion subunits of influenza A virus hemagglutinin (HA) are known to block viral fusion^{19,20}. Notably, the anti-HA antibodies recognize only the fusion subunit, whereas 16F6 and KZ52 bind both the fusion subunit and the receptor-binding subunits of the glycoprotein and physically anchor them together. Hence, the shared epitope of 16F6 and KZ52 suggests a unique structural strategy by which antibodies inhibit viral infection.

In summary, we have demonstrated efficacy *in vitro* and *in vivo* of the first antibody shown to neutralize Sudan virus, and we have crystallized it in complex with the oligomeric, prefusion SUDV (Gulu) GP_{1,2}. This structure and accompanying mechanistic analysis reveal new insights into ebolavirus entry and demonstrate that antibodies elicited in two unique host species by different scenarios bind overlapping epitopes and function at a similar post-entry step. These overlapping epitopes may indicate a crucial site for neutralization of ebolaviruses. Our work further suggests that for viruses in general, successful immunotherapy and vaccine design may depend on targeting antibodies that anchor glycoprotein subunits together and prevent the conformational changes required for fusion.

Accession code. Coordinates and structure factors have been deposited into the Protein Data Bank under accession code 3S88.

Note: Supplementary information is available on the Nature Structural & Molecular Biology website.

ACKNOWLEDGMENTS

We thank D. Burton and A. Hessel (The Scripps Research Institute, TSRI) for KZ52, M. Whitt (University of Tennessee Health Science Center) and D. Lyles (Wake Forest University School of Medicine) for anti-VSV IgG 23H12, J. Cunningham (Brigham and Women's Hospital) for rabbit anti-GP1 polyclonal antibody and I. Wilson of TSRI for critical reading of the manuscript. We would also like to thank C. Corbaci (TSRI) for assistance in figure preparation and the staff of the Advanced Photon Source Beamline 19-ID and the Advanced Light Source Beamlines 8.2.2 and 8.3.1 for assistance and for the use of their US Department of Energy-supported facilities. E.O.S. wishes to acknowledge US National Institutes of Health (NIH) grant U01 AI070530, the Skaggs Institute for Chemical Biology, a Career Award in the Biomedical Sciences and an Investigator in the Pathogenesis of Infectious Disease Award from the Burroughs Wellcome Fund. K.C. acknowledges support from NIH grants R01 AI088027 and R21 AI082437 and from institutional funds of the Albert Einstein College of Medicine.

A.C.W. was supported by NIH training grants T32 GM007288 and T32 AI070117. Y.K. acknowledges support from NIH R01 AI055519 and membership within and support from the Region V 'Great Lakes' Regional Center for Excellence for Biodefense and Emerging Infectious Diseases Research (RCE) Program (NIH award 2 U54 AI057153). J.M. Dye wishes to acknowledge support from the Defense Threat Reduction Agency (DTRA K.K0001_07_RD_B). Opinions, interpretations, conclusions and recommendations are those of the authors and are not necessarily endorsed by the US Army.

AUTHOR CONTRIBUTIONS

J.M. Dias determined the crystal structure, S.B. continued refinement and M.L.F. engineered SUDV GP_{1,2} for crystallization. A.I.K., E.K., S.E.Z., M.A.M. and J.M. Dye raised 16F6 and designed and conducted BSL-4 neutralization and protection experiments. D.M.A., E.O.S., A.C.W. and K.C. designed and carried out cathepsin cleavage and VSV neutralization experiments. D.M.A., E.O.S., P.H. and Y.K. designed and conducted attachment and entry experiments. J.M. Dias, J.M. Dye, D.M.A., S.B., A.K., K.C., P.H., Y.K. and E.O.S. analyzed results. J.M. Dye, K.C., Y.K. and E.O.S. supervised the research. J.M. Dias, J.M. Dye and E.O.S. wrote the manuscript.

COMPETING FINANCIAL INTERESTS

The authors declare no competing financial interests.

Published online at <http://www.nature.com/nsmb/>.

Reprints and permissions information is available online at <http://www.nature.com/reprints/index.html>.

- Sanchez, A. & Rollin, P.E. *Virus Res.* **113**, 16–25 (2005).
- Okware, S.I. *et al. Trop. Med. Int. Health* **7**, 1068–1075 (2002).
- Maruyama, T. *et al. J. Infect. Dis.* **179** Suppl 1, S235–S239 (1999).
- Takada, A. *et al. J. Virol.* **77**, 1069–1074 (2003).
- Wilson, J.A. *et al. Science* **287**, 1664–1666 (2000).
- Shahhosseini, S. *et al. J. Virol. Methods* **143**, 29–37 (2007).
- Yu, J.S. *et al. J. Virol. Methods* **137**, 219–228 (2006).
- Volchkov, V.E., Feldmann, H., Volchkova, V.A. & Klenk, H.D. *Proc. Natl. Acad. Sci. USA* **95**, 5762–5767 (1998).
- Jeffers, S.A., Sanders, D.A. & Sanchez, A. *J. Virol.* **76**, 12463–12472 (2002).
- Dube, D. *et al. J. Virol.* **83**, 2883–2891 (2009).
- Hood, C.L. *et al. J. Virol.* **84**, 2972–2982 (2010).
- Lee, J.E., Fusco, M.L., Hessel, A.H., Burton, D.R. & Saphire, E.O. *Acta Crystallogr. D* **65**, 1162–1180 (2009).
- Lee, J.E. *et al. Nature* **454**, 177–182 (2008).
- Halfmann, P. *et al. Proc. Natl. Acad. Sci. USA* **105**, 1129–1133 (2008).
- Chandran, K., Sullivan, N.J., Felbor, U., Whelan, S.P. & Cunningham, J.M. *Science* **308**, 1643–1645 (2005).
- Schornerberg, K. *et al. J. Virol.* **80**, 4174–4178 (2006).
- Weissenhorn, W., Carfi, A., Lee, K.H., Skehel, J.J. & Wiley, D.C. *Mol. Cell* **2**, 605–616 (1998).
- Malashkevich, V.N. *et al. Proc. Natl. Acad. Sci. USA* **96**, 2662–2667 (1999).
- Ekiert, D.C. *et al. Science* **324**, 246–251 (2009).
- Sui, J. *et al. Nat. Struct. Mol. Biol.* **16**, 265–273 (2009).

